Structure and Dynamics of Phosphoranyl Radicals. A Single-Crystal Electron Spin Resonance Study†

J. H. H. Hamerlinck,* P. Schipper, and H. M. Buck

Contribution from the Department of Organic Chemistry, Eindhoven University of Technology, Eindhoven, The Netherlands. *Received March 23, 1982*

Abstract: The structures of phosphoranyl P^V radicals have been obtained from single-crystal ESR measurements. The radicals were prepared by X-irradiation or UV laser irradiation of their parent compounds. It is shown that phosphorus adopts a P^V trigonal-bipyramidal (TBP) structure in these radicals. The unpaired electron is located either in an apical (a) or equatorial (e) position of the TBP as a fifth ligand. Since both TBP-a and TBP-e configurations are formed in one sample of X-irradiated $HP(OCH_2CH_2)_3N^+BF_4^-$, comparison of the two stereoisomers shows that the amount of s character in the apical bonds is reduced in comparison with the equatorial bonds. Besides these TBP-a and TBP-e structures the octahedral P^{VI} geometry of $ClP(O_2C_6H_4)_2^-\cdot$ is established, with the unpaired electron and chlorine in the axial axis. Intramolecular ligand reorganization in phosphoranyl radicals is studied in a single crystal, which reveals the exact mode of permutation: a Berry pseudorotation, with the unpaired electron acting as the pivot. It is found that the intermediate square-pyramidal (SP) geometry in this process lies only slightly above the TBP-e structure in energy.

In recent years the structure of phosphoranyl radicals ($PX_4\cdot$) has received much attention. These radicals have been suggested to act as intermediates in the reaction of free radicals, e.g., alkoxy and alkyl radicals, in the presence of trivalent phosphorus compounds, giving products primarily by either α- or β-scission processes[1] as given in Scheme I. Two important overall processes are observed, oxidation and substitution. A number of ESR studies have shown that phosphoranyl radicals are in fact formed in these systems.[2] Initially a TBP structure was assigned with the unpaired electron in an equatorial position acting as a fifth (phantom) ligand (TBP-e).[3] This is based on the isotropic phosphorus hyperfine

coupling (hfc) obtained from liquid-phase ESR work and theoretical predictions. For example, by use of the unrestricted Hartree–Fock method within a 4-31G basis set the optimized TBP-a structure of $PH_4\cdot$ is calculated to be about 15 kcal/mol above the optimized TBP-e form, while the C_{4v} square-pyramidal (SP) structure with an axial electron lies 34 kcal/mol above the TBP-e geometry.[4] Moreover, the tetrahedral (C_{3v}) form is found to be 57.5 kcal/mol above the TBP-e form.

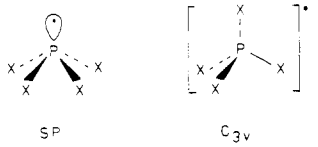

The limitations of solution ESR were recognized when anisotropic ESR studies, which give information about the P_{3p} orbital involved, became available. On the basis of a single-crystal ESR study of $Cl_3PO^-\cdot$[5] and $PF_4\cdot$[6] in which the unpaired electron is

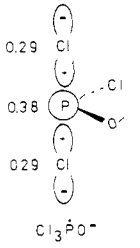

† This work was abstracted from the Ph.D. dissertation of J.H.H.H., Eindhoven University of Technology, 1982.

Scheme I. Formation of α- and β-Scission Products from TBP-e Phosphoranyl Radicals

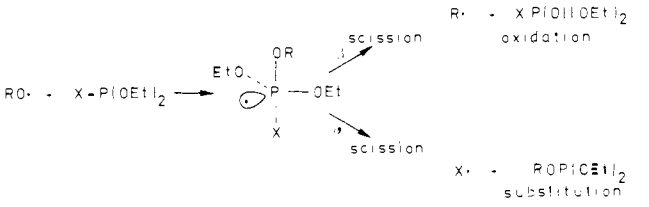

Scheme II. Isomerization of a TBP-e Phosphoranyl Radical via a σ^* Intermediate

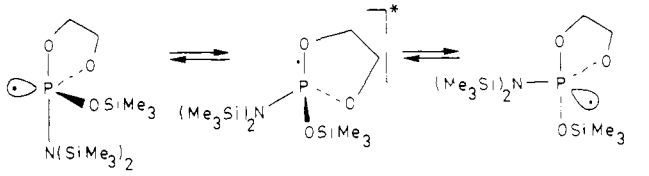

assumed to be delocalized in a σ^* orbital of the apical ligand linkages in the TBP structure, it has been suggested that the TBP-e structure is only a poor description of the real structure of the phosphoranyl radical, and a "Rundle three-center" bonding has been proposed. Analogously the unpaired electron in the $Ph_3PCl\cdot$ radical, which possesses a C_{3v} structure, is also believed to reside in a σ^* P–Cl orbital.[7] accounting for the high spin density found on chlorine and the fact that the ^{31}P tensor is parallel to the ^{35}Cl tensor. In recent literature this σ^*-C_{3v} structure has been adopted as an intermediate in ligand exchange processes of nonrigid TBP-e phosphoranyl radicals in solution. An example for isomerization via a σ^* intermediate is depicted in Scheme II.[8]

In comparison with the σ^*-C_{3v} structure, with a quite large hfc due to the halogen ligand, the assignment of a C_{4v} structure to $PF_5^-\cdot$ in γ-irradiated hexafluorophosphate[9] in the solid state is

(1) Bentrude, W. G.; Del Alley, W.; Johnson, N. A.; Murakami, M.; Nishikida, K.; Tan, H. W. *J. Am. Chem. Soc.* **1977**, *99*, 4383.
(2) Krusic, P. J.; Mahler, W.; Kochi, J. K. *J. Am. Chem. Soc.* **1972**, *94*, 6033.
(3) Davies, A. G.; Parrott, M. J.; Roberts, B. P. *J. Chem. Soc., Chem. Commun.* **1974**, 973.
(4) Howell, J. M.; Olsen, J. F. *J. Am. Chem. Soc.* **1976**, *98*, 7119.
(5) Gillbro, T.; Williams, F. *J. Am. Chem. Soc.* **1974**, *96*, 5032.
(6) Hasegawa, A.; Ohnishi, K.; Sogabe, K.; Miura, M. *Mol. Phys.* **1975**, *30*, 1367.
(7) Berclaz, T.; Geoffroy, M.; Lucken, E. A. C. *Chem. Phys. Lett.* **1975**, *36*, 677.
(8) Roberts, B. P.; Singh, K. *J. Chem. Soc., Chem. Commun.* **1979**, 980.

0002-7863/83/1505-0385$01.50/0

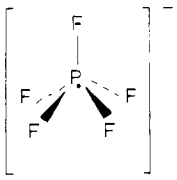

most remarkable, since in spite of the obvious similarity between the C_{3v} and C_{4v} structures both with an axially located electron, a near-zero hfc of the fifth ligand in axial position in $PF_5^{-\cdot}$ has been tentatively proposed as a general rule,[10-12] e.g., in $SF_5\cdot$ and $PCl_5^{-\cdot}$.

The aim of this study is to determine the various geometries that phosphoranyl radicals are able to adopt and the dynamic behavior of these intermediates. Since it is apparent that the most important information about the electronic nature of these radicals is associated with the direction of the P_{3p} orbital involved, single crystals are necessary. Moreover, the radicals have to be formed in such way that their ESR spectra can be correlated with the X-ray analysis results of their precursors. This has been achieved by selective bond scission of P^V phosphoranes or specific electron addition to P^{IV} phosphate upon X-irradiation of single crystals, resulting in a reliable description of the radicals **1a–7a** and **7b**. In one case (**8a**), a P^{VI} radical is obtained. The ESR parameters are given in Table I. The spin densities on phosphorus and the other nuclei (^1H, ^{14}N, ^{35}Cl, and ^{37}Cl) were calculated from the isotropic hfc (a_{iso}) and the anisotropic hfc (B) as indicated. The detailed elaboration is given in the Appendix.

Results

A. **Rigid Structures. (I) Phosphorus in a TBP Structure with the Unpaired Electron Located in an Equatorial Position (TBP-e). 1,6-Dioxa-4,9-diaza-5-phospha(5-P^V)spiro[4.4]nonan-5-yl Radical (1a).** Single crystals of 1,6-dioxa-4,9-diaza-5-phospha(5-P^V)-spiro[4.4]nonane (**1**), which are grown by slow crystallization from anhydrous benzene, are monoclinic with space group $C2/c$ and have a crystallographic 2-fold axis along the P–H bond.[13] In **1** the P atom is in a TBP configuration with the adjacent H and nitrogens in the equatorial positions. Four molecules are in a unit cell (Figure 1).[14] By means of the rotating crystal method[15] using Cu K_α radiation, the crystal needle axis was identified to be the crystallographic c axis. The radical was generated by X irradiation at room temperature. An X-irradiated crystal glued on a small quartz rod was studied in three planes, i.e., a^*b, bc, and a^*c planes. The noncrystallographic a^* axis is chosen perpendicular to the bc plane. X irradiation of **1** gives rise to the ESR spectra (Figure 2) ascribed to **1a**, only one ^{31}P doublet is observed, and no additional couplings have been detected.[16] The angular variations are shown in Figure 3a–c. Rotating the single crystal of **1** around the crystallographic c axis reveals the maximum anisotropy $a_{P\parallel}$ to be perpendicular to this axis. Similarly for a rotation about the a^* axis it was found that $a_{P\parallel}$ is perpendicular to the a^* axis. This corresponds with the direction of the P–H linkage in its precursor as determined by X-ray diffraction analysis (Figure 1). From Figure 2 it is seen that the hfc is axially symmetric. The same applies for the g tensor: $g_\parallel = 1.988$ and $g_\perp = 2.005$. It was found that X irradiation and UV laser irradiation ($\lambda = 248$ nm) at 77 K of a powdered sample of **1** gives rise to the same radical. The parameters derived from the powder spectra agreed nicely with those obtained from the single-crystal measurements; only the directional information is lacking.

The orbital in which the unpaired electron resides is directed along the initial P–H linkage. Obviously the radical **1a** is generated by P–H bond scission. Therefore the structure of **1a** has to be described as a nearly perfect TBP with the unpaired electron and the nitrogen ligands in the equatorial positions and the oxygen ligands in the apical positions. From the anisotropic values of

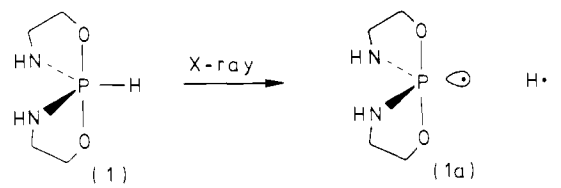

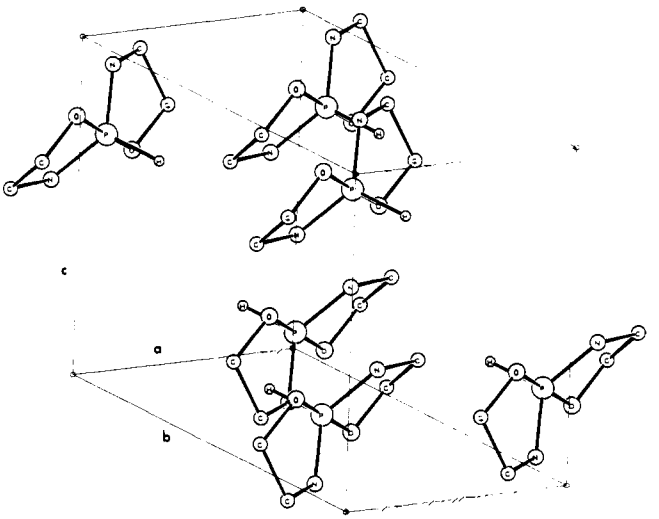

Figure 1. ORTEP drawing of the unit cell of **1**.

Figure 2. ESR spectra of **1a**: (a) powder spectrum, (b) single-crystal ESR spectrum, H_0 parallel to the c axis, (c) single-crystal ESR spectrum, H_0 parallel to the b axis.

(9) Mishra, S. P.; Symons, M. C. R. *J. Chem. Soc., Chem. Commun.*, **1974**, 279.
(10) Morton, J. R.; Preston, K. F.; Strach, S. J. *J. Magn. Reson.* **1980**, *37*, 321.
(11) Hasegawa, A.; Williams, F. *Chem. Phys. Lett.* **1977**, *45*, 275.
(12) Mishra, S. P.; Symons, M. C. R. *J. Chem. Soc., Dalton Trans.* **1976**, 139.
(13) Meunier, P. F.; Day, R. O.; Devillers, J. R.; Holmes, R. R. *Inorg. Chem.* **1978**, *17*, 3270.
(14) The ORTEP drawings were kindly prepared by Dr. G. J. Visser, Computing Centre of the Eindhoven University of Technology, The Netherlands.
(15) Milburn, G. H. W. "X-ray Crystallography"; Butterworth: London, 1973. See also the appendix.
(16) Hamerlinck, J. H. H.; Schipper, P.; Buck, H. M. *J. Chem. Soc., Chem. Commun.* **1981**, 104.

Table I. ESR Parameters of Radicals 1a-8a and 7b

compd		$a_{\parallel}$, G	$a_{\perp}$, G	a_{iso}, G	B, G	ρ_s[a]	ρ_p[a]	$g_{\parallel}$	$g_{\perp}$
1a	^{31}P	893	735	788	53	0.22	0.49	1.988	2.005
2a	^{31}P	960	808	859	50	0.24	0.47	1.983	2.008
3a	^{31}P	1061	869	933	64	0.26	0.60		
4a	^{31}P	1167	1005	1059	54	0.29	0.51		
5a	^{31}P	715	606	642	36	0.18	0.35		
	^{14}N	26.3	24.0	24.8	0.8	0.05 (2 N)			
6a	^{31}P	886	776	813	37	0.22	0.35	1.988	2.005
	^{1}H	5	5	5		0.01 (1 H)			
7a	^{31}P	1120	930	993	63	0.27	0.61		
7b	^{31}P	888	753	798	45	0.21	0.43	1.988	2.005
	^{14}N	21.2	22.7	22.2	0.5	0.04 (1 N)			
8a	^{31}P	1400	1289, 1263	1317	42	0.36	0.40	1.988	2.008, 2.011
	^{35}Cl	47	23, 24	31	8	0.02 (1 Cl)	0.16 (1 Cl)		
	^{37}Cl	43	22, 22	29	7	0.02	0.16		

[a] Reference values used for calculation of $\rho_s = a_{iso}/a_0$ and $\rho_p = B/B_0$. Nuclear a_0 (G), B_0 (G):[17] ^{31}P 3640, 103; ^{1}H 508; ^{14}N 552, 17; ^{35}Cl 1680, 50; ^{37}Cl 1395, 42.

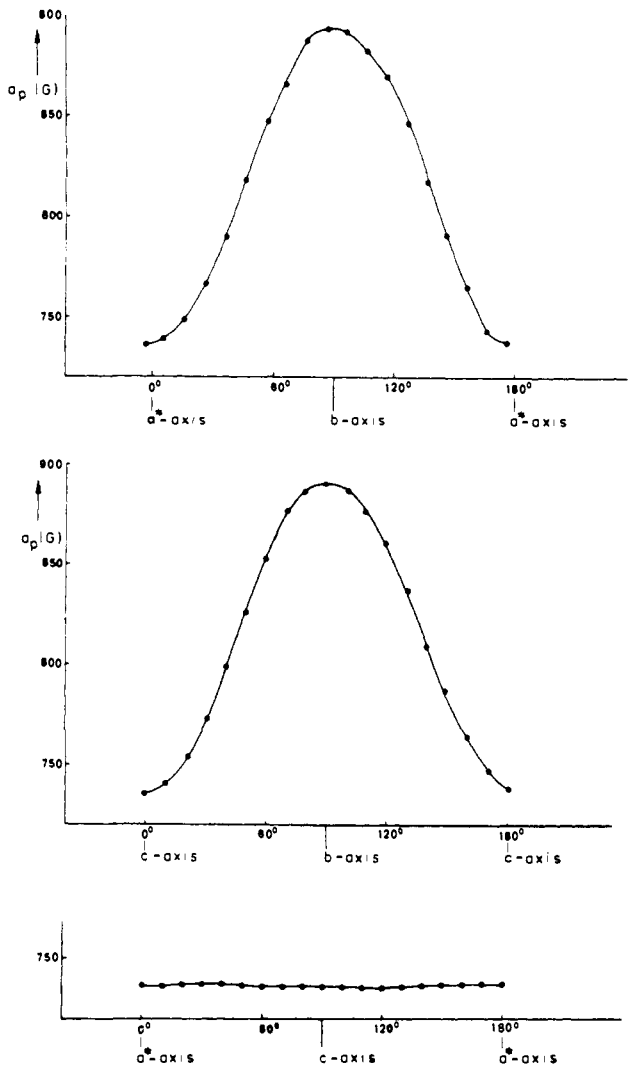

Figure 3. Angular variation of a_p of **1a** (a) in the a^*b plane (top), (b) in the bc plane (center), (c) in the a^*c plane (bottom).

the phosphorus hfc $a_{P\parallel}$ = 893 G, $a_{P\perp}$ = 735 G, and the $a_{P\text{-iso}}$ is calculated[17] to be 788 G. From the line width the ^{14}N coupling was estimated to be less than 5 G. The remaining spin density will be distributed over the apical oxygen ligands. These values indicate a phosphorus 3s spin density of 0.22 and a 3p spin density of 0.49, resulting in a total spin density of 0.71 on phosphorus in an sp^2 hybrid orbital.

(17) Atkins, P. W.; Symons, M. C. R. "The Structure of Inorganic Radicals"; Elsevier: Amsterdam, 1967.

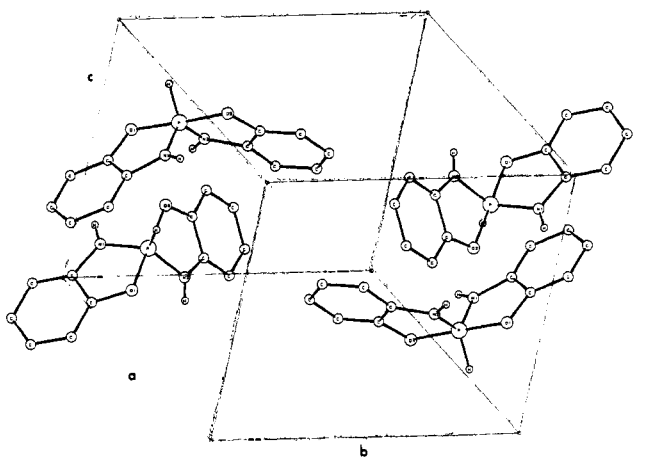

Figure 4. ORTEP drawing of the unit cell of **2**.

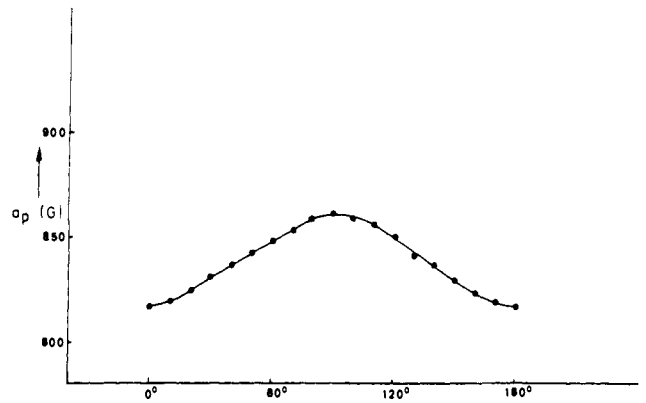

Figure 5. Angular variation of a_p of **2a** on rotation about the c axis.

1,6-Dioxa-4,9-diaza-2,3:7,8-dibenzo-5-phospha(5-P^V)spiro-[4.4]nona-2,7-dien-5-yl Radical (2a). Single crystals of 1,6-dioxa-4,9-diaza-2,3:7,8-dibenzo-5-phospha(5-P^V)spiro[4.4]nona-2,7-diene (**2**) were prepared[13] by slow crystallization from anhydrous benzene. Compound **2** crystallizes in the monoclinic space group $P2_1/c$ with four molecules in the unit cell (Figure 4) and with an approximate 2-fold axis along the P–H bond. By use of the rotating crystal method the c axis was identified in the crystal. The radical was generated by X irradiation at room temperature. In **2** phosphorus adopts a TBP structure with the adjacent hydrogen and the nitrogen atoms in the equatorial positions.

X irradiation of **2** generates the phosphoranyl radical assigned to **2a**.[16] At least two sites are expected. The principal a_p values were easily obtained from an X-irradiated powdered sample. When the crystal is rotated about the crystallographic c axis only one site is observed, as is shown in Figure 5. This is consistent with the crystal symmetry. From the maximum value of a_p

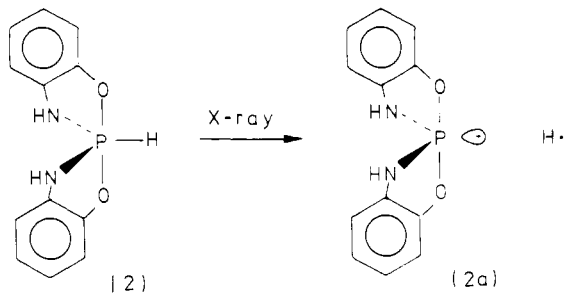

(2) (2a)

obtained from Figure 5 together with the $a_{P\parallel}$ value derived from the powder spectrum (Figure 6) it is calculated that the angle between $a_{P\parallel}$ and the crystallographic c axis amounts to 35°. This is in excellent agreement with the angle of the P–H bond with the c axis, which has been determined to be 36°. In this radical also, the unpaired electron is directed along the initial P–H bond. Therefore **2a** possesses a TBP structure with the unpaired electron and the nitrogen atoms in equatorial positions and the oxygens in apical positions. The axially symmetric ^{31}P hfc, $a_{P\parallel}$ = 960 G, $a_{P\perp}$ = 808 G, give $a_{P\text{-}iso}$ = 859 G and the anisotropic contribution is 50 G. This indicates a phosphorus 3s spin density of 0.24 and a 3p spin density of 0.47, resulting in a 0.71 spin density on phosphorus in an sp^2 hybrid orbital. From the line width it was estimated that a_N < 5 G (not resolved). The remaining spin density will be distributed over the apical ligands.

Analogous TBP-e Structures. Analogous TBP-e structures were obtained for the following X-irradiated compounds: **3**, **4**, and **5**.

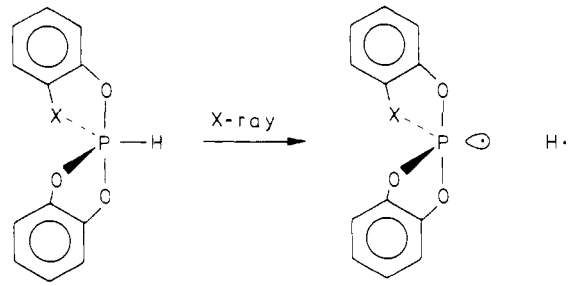

(3) X = NH (3a) X = NH
(4) X = O (4a) X = O

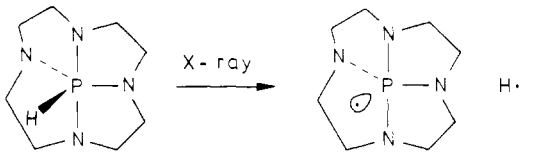

(5) (5a)

From X-ray diffraction analysis it is known that **3** and **4** possess a nearly perfect TBP structure with the P–H bond located equatorially.[18,19] The a_P values of the TBP-e radical structures are compiled in Table I. The structure of **5a**, which will be described in detail in Section B because of its interesting dynamic behavior, is also TBP-e and was studied both in powder and single crystal form. Its ^{31}P hfc values are $a_{P\parallel}$ = 715 G and $a_{P\perp}$ = 606 G and hfc of $a_{N\parallel}$ = 26.3 G and $a_{N\perp}$ = 24.0 G due to the two nitrogen atoms in the apical positions, while the equatorial nitrogens did not have resolved hfc (<5 G from line width).

(II) Phosphorus in a TBP Structure with the Unpaired Electron Located in an Apical Position (TBP-a). Thiophosphate *O,O,O*-Triester of Methyl β-D-Ribopyranoside Radical Anion (6a). The

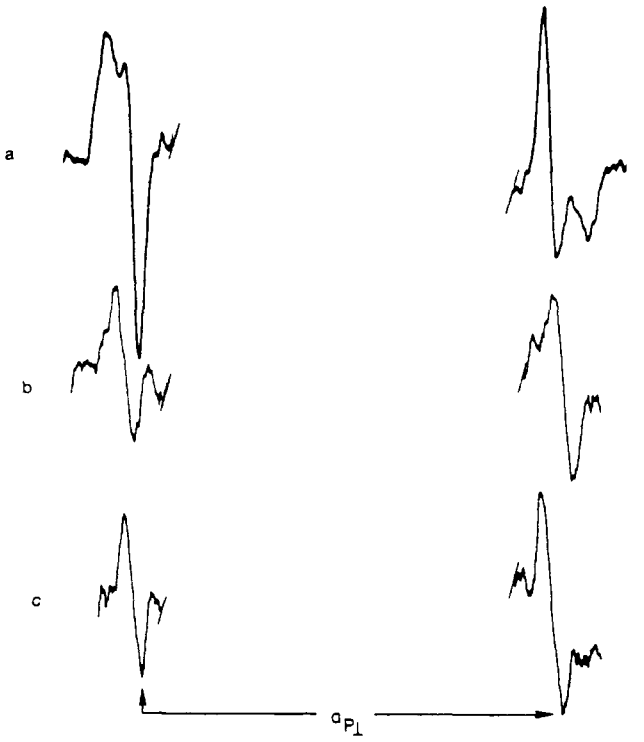

Figure 6. ESR spectra of **2a**: (a) powder spectrum, (b) maximum a_P value on rotation around the c axis, (c) $a_{P\perp}$ (rotation around the c axis).

ESR spectrum of this radical has recently been published in detail.[20] It is generated by X irradiation or UV laser irradiation at 77 K of a single crystal of thiophosphate *O,O,O*-triester of methyl β-D-ribopyranoside. Correlation of the X-ray diffraction results with the anisotropic ESR spectra recorded along the crystallographic axes reveals that the radical anion **6a** has been

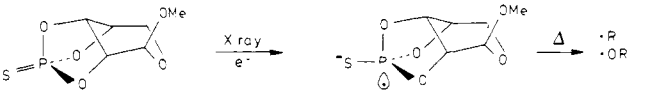

(6) (6a)

generated by electron capture at phosphorus. It is found that the unpaired electron resides in an apical position in the TBP structure with the O–P–· angle being 162°. From the anisotropic values of the ^{31}P hfc, $a_{P\parallel}$ = 886 G and $a_{P\perp}$ = 776 G, the $a_{P\text{-}iso}$ is calculated to be 813 G. These values indicate a phosphorus 3s spin density of 0.22 and a 3p spin density of 0.35, resulting in a total spin density of 0.57 located on phosphorus in an apical position. A superimposed hfc of 5 G is due to the hydrogen in quasi-apical position. This hfc is isotropic and probably has a negative sign because it is the result of spin polarization. The remaining spin density will be distributed over the equatorial ligands.

Its TBP structure will be stabilized by the five-membered rings that span apical–equatorial positions, placing the six-membered ring diequatorially.[21] Electronically, it is conceivable that the negative sulfur ligand favors the equatorial position in this rigid framework. The central features of the ESR spectrum due to alkyl and alkoxy radicals are analogous to those reported for comparable sugar radicals[22] resulting from bond scission. *The results suggest that in irradiated nucleic acid polymers (DNA) electrons are trapped by phosphorus, giving rise to a phosphorus centered radical that subsequently induces bond break by α or β scission, generating thermodynamically more stable sugar and base radicals.*

(III) TBP-e and TBP-a Isomers. $\cdot\overline{P(OCH_2CH_2)_3N}^+BF_4^-$

(18) Wunderlich, H.; Wussow, H. G. *Acta Crystallogr., Sect. B* **1978**, *34*, 2663.
(19) Clark, T. E.; Day, R. O.; Holmes, R. R. *Inorg. Chem.* **1979**, *18*, 1653.
(20) Hamerlinck, J. H. H.; Schipper, P.; Buck, H. M. *J. Chem. Phys.* **1982**, *76*, 2161.
(21) Hudson, R. F.; Brown, C. *Acc. Chem. Res.* **1972**, *5*, 204.
(22) Locher, S. E.; Box, H. C. *J. Chem. Phys.* **1980**, *72*, 828.

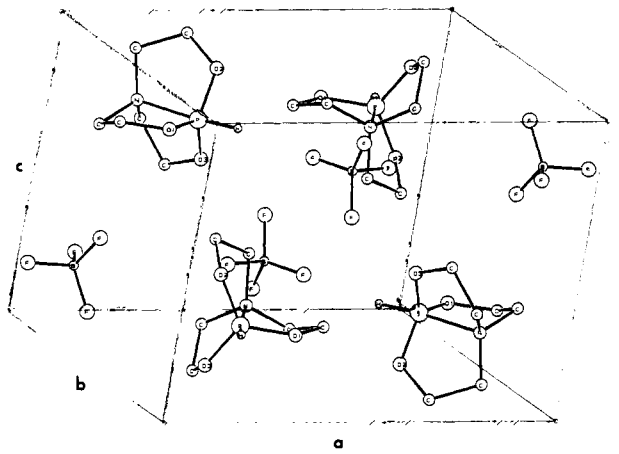

Figure 7. ORTEP drawing of the unit cell of **7**.

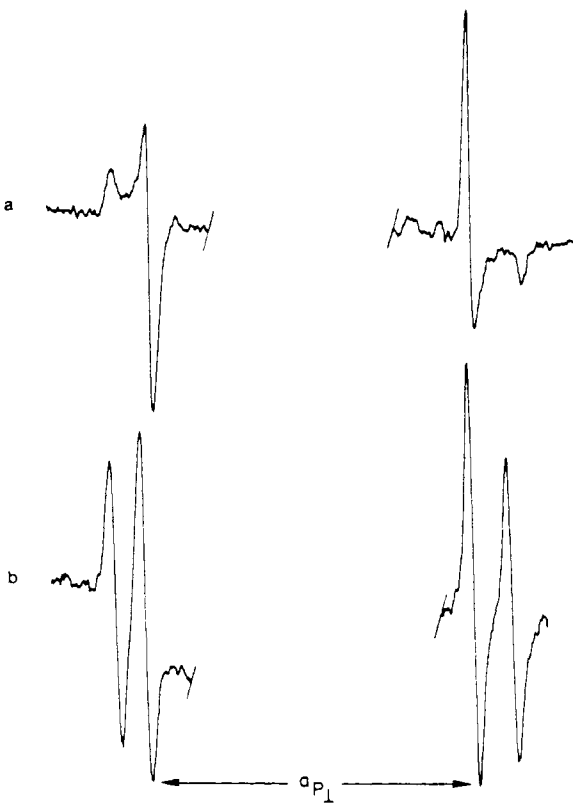

Figure 8. ESR spectra of **7a**: (a) powder spectrum, (b) single-crystal spectrum.

Radical. A single crystal of $\overline{HP(OCH_2CH_2)_3N^+BF_4^-}$ (**7**) was grown by slow crystallization from anhydrous acetonitrile.[23] It crystallizes in the orthorhombic space group *Pnam* with four molecules in the unit cell (Figure 7). In **7** the P atom possesses a TBP configuration with nitrogen and the adjacent hydrogen in the apical positions as revealed by X-ray crystallography. Crystal alignment was performed by the Laue back-reflection method by use of Cu K_α radiation.[24] The irradiations were performed at 77 K on a crystal of **7** with either X-ray or UV laser (λ = 193 or 248 nm). X irradiation of a single crystal of **7** at liquid nitrogen temperature (77 K) yields the spectrum of radical **7a** exclusively, with $a_{P_\parallel}$ = 1120 G and $a_{P_\perp}$ = 930 G, while ^{14}N splitting is not resolved.[25] The formation of **7a** and **7b** (vide infra) is given in Scheme III.

(23) Clardy, J. C.; Milbrath, D. S.; Springer, J. P.; Verkade, J. G. *J. Am. Chem. Soc.* **1976**, *98*, 623.
(24) Cullity, B. D. "Elements of X-ray Diffraction"; Addison-Wesley: London, 1959.
(25) Hamerlinck, J. H. H.; Schipper, P.; Buck, H. M. *J. Chem. Soc., Chem. Commun.* **1981**, 1149.

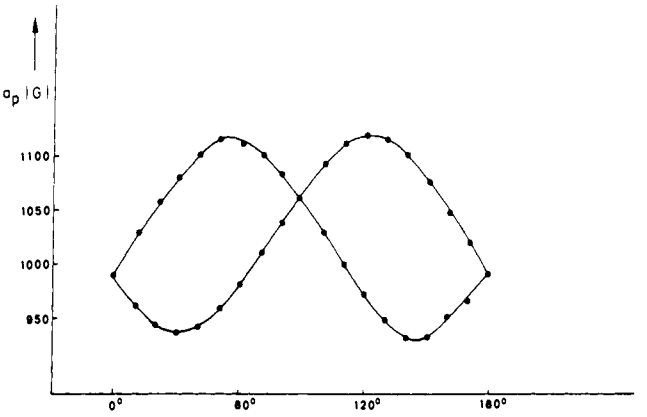

Figure 9. Angular variation of a_P of **7a** in the *ab* plane.

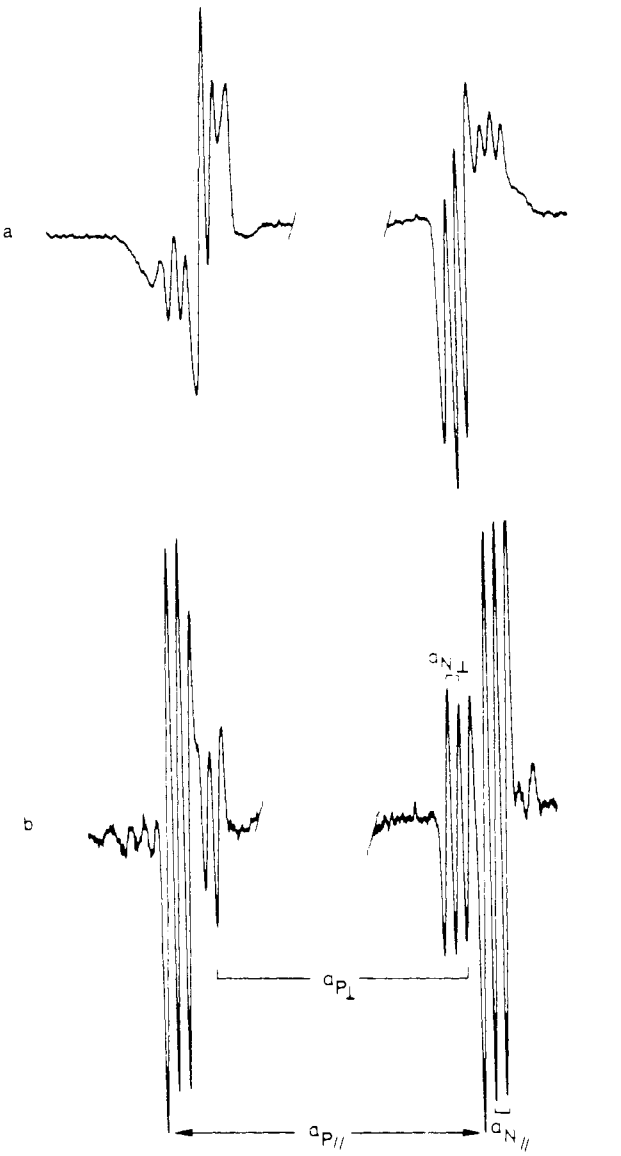

Figure 10. ESR spectra of **7b**: (a) powder spectrum, (b) single-crystal spectrum.

On rotation about the crystallographic *c* axis two orientations are present with an angle between their $a_{P_\parallel}$ components of 70 ± 2° (Figure 8). The angular variations of ^{31}P hfc are shown in Figure 9. When the temperature is raised, these signals start to disappear irreversibly at 193 K and those of **7b** become apparent. Two radicals with an angle between their $a_{P_\parallel}$ components of 90 ± 2° are present on rotation about the crystallographic *c* axis (Figure 10).[26] The occurrence of differently oriented radicals

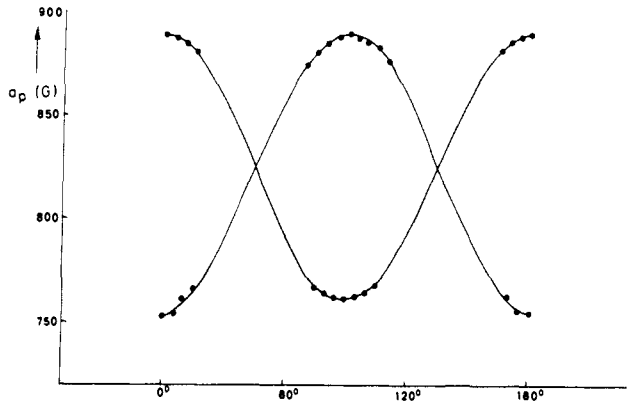

Figure 11. Angular variation of a_P of **7b** in the *ab* plane.

Scheme **III.** Formation of 7a and 7b under X Irradiation and UV Photolysis

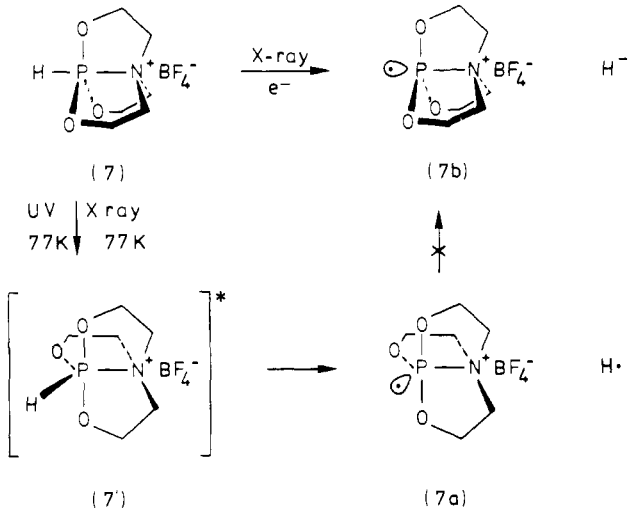

is consistent with the X-ray diffraction analysis results of precursor **7** that also show two orientations in the unit cell (Figure 7). By means of the Laue back-reflection method it was shown that the $a_{P\parallel}$ is oriented approximately along the initial P–H linkage, the N–P–· angle being 168°. Furthermore one ^{14}N hfc is present. Because of severe overlap of the two sites, the ESR spectra of the irradiated single crystal could only be analyzed in the regions of maximum separation (Figure 11). Nevertheless, on rotation about the *c* axis the principal values of **7b** are obtained, as was checked by comparison with the powder ESR spectrum (Figure 10).

In the plane perpendicular to the crystal mounting axis (*c* axis), the directions of $a_{P\parallel}$ of **7a** and **7b** differ 35° or the complementary angle of 55°, which cannot be assigned uniquely due to the presence of two orientations in the unit cell (Figure 7). Surprisingly, UV laser irradiation at 77 K of a crystal of **7** generates only radical **7a** without any trace of **7b** on warming. The direction of $a_{P\parallel}$ of **7b** is nearly along the P–N axis. Therefore it is concluded that radical **7b** possesses a TBP structure with the unpaired electron and nitrogen in the apical positions. The anisotropic ^{31}P hfc, $a_{P\parallel}$ = 888 G and $a_{P\perp}$ = 753 G, results in a spin density of 0.21 in the phosphorus 3s orbital and 0.43 in its 3p orbital, indicating that the unpaired electron resides in an sp^2 hybrid orbital of phosphorus. The ^{14}N hfc, $a_{N\parallel}$ = 21.2 G, $a_{N\perp}$ = 22.7 G, and $a_{N\text{-iso}}$ = 22.2 G, indicates a spin density of 0.05 in the 2s orbital of nitrogen. The anisotropic contribution (0.5 G) can be attributed to dipole–dipole interaction. Apparently, the remaining spin density is distributed over the equatorial oxygen ligands. It is found that the directions of the $a_{P\parallel}$ components of **7b** and **7a** differ by 35° or 55°, both angles inferring a TBP-e geometry for **7a**.

Furthermore, the a_P values of **7a** are consistent with those found for the closely related phosphoranyl radical **3a** generated by X irradiation of **3**, which is known to possess a nearly perfect TBP structure as inferred from X-ray diffraction analysis.

From the anisotropic ^{31}P hfc values obtained for **7a**, $a_{P\text{-iso}}$ = 993 G is calculated, indicating the phosphorus 3s spin density is 0.27, while the anisotropic contribution places 0.61 of the spin density in its 3p orbital, which gives a total spin density of 0.88 on phosphorus. It is generally accepted that the primary process resulting from the interaction of high energy quanta and a molecule is the ejection of an inner electron. This electron can be trapped in the matrix, or it may return to the parent cation.[17] The resulting molecule, which is in a high vibrational ground state, will frequently have sufficient energy to undergo homolytic bond rupture. Furthermore, it is observed that the trapped electrons are mobilized on warming or by UV irradiation, giving rise to reaction with the medium or the substrate.

This is illustrated in Scheme III for the formation of **7a** and **7b** from irradiated **7**. Primarily, compound **7** is ionized. Return of an electron generates a molecule that is in a high vibrational ground state (**7'***). Subsequently, **7'*** undergoes P–H bond cleavage with retention of configuration, producing **7a**. Electronically, structure **7'** with the hydrogen atom in equatorial position is favored over **7** with the hydrogen atom in apical position. In contrast, the strain energy in structure **7'** is enhanced with respect to that of **7**. However, the latter factor may be less important in **7'*** since in this high vibrational gound state the bond lengths are increased. Therefore, in **7'*** the electronic factor has become dominant. It appears that the concentration of **7a** increases on warming. Therefore, the return of an electron to the parent cation is a thermodynamically controlled process.

It is conceivable that trapped electrons attack **7** at higher temperature, generating a radical anion that produces **7b** by subsequent loss of H^- from the apical axis of the TBP. It has been confirmed that trapped electrons are involved in the formation of **7b** by an experiment in which compound **7** is X irradiated at 77 K, showing **7a**. Subsequently, this sample is UV irradiated at 77 K, which leads to loss of **7a**. On warming the concentration of **7a** is increased, whereas radical **7b** does not show up at all. Obviously, UV irradiation delocalizes the trapped electrons that attack both **7a**, leading to a diamagnetic product, and **7**, resulting in **7b**. However, in this experiment **7b** is not detected, simply because this radical is lost upon UV irradiation, as was proven independently. It is concluded that homolytic P–H bond rupture is favored in an equatorial position of the TBP, whereas this process is inhibited in an apical position. In contrast, loss of H^- takes place in an apical position preferentially.

(IV) **Phosphorus in an Octahedral P^{VI} Geometry with the Unpaired Electron in Axial Position. 2-Chloro-2,2'-spirobis(1,3,2-benzodioxaphosphol)-2-yl Radical Anion (8a).** A single crystal of 2-chloro-2,2'-spirobis(1,3,2-benzodioxaphosphole)[27] (**8**) was grown by slow crystallization from 1:1 benzene–hexane. It crystallizes in the monoclinic $P2_1/n$ space group with four molecules in the unit cell (Figure 12) and has a noncrystallographic 2-fold axis about the P–Cl bond. Its structure is 72% displaced from TBP to rectangular pyramidal along the Berry exchange coordinate. By means of the rotating crystal method, using Cu K_α radiation the crystallographic *a* axis has been identified. The radical was generated by X irradiation at room temperature.

X irradiation of **8** at room temperature gives rise to the ESR spectrum of radical **8a**.[28] On rotation of the crystal around the

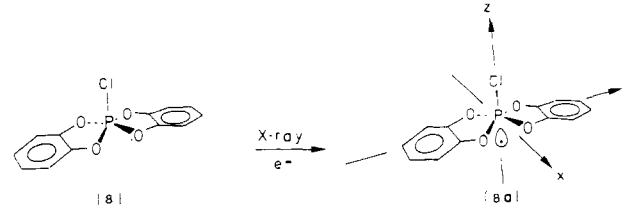

(26) Hamerlinck, J. H. H.; Schipper, P.; Buck, H. M.; *J. Am. Chem. Soc.* **1980**, *102*, 5679.

(27) Brown, R. K.; Holmes, R. R.; *Inorg. Chem.* **1977**, *16*, 2294.

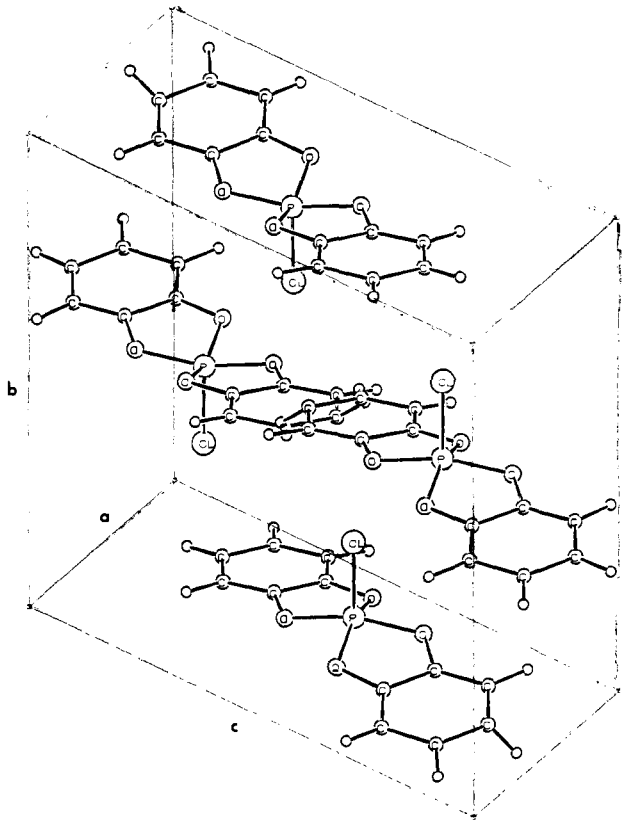

Figure 12. ORTEP drawing of the unit cell of **8**.

crystallographic *a* axis, only one site is detected (Figure 13). The angular variation of the ^{31}P and ^{35}Cl hfc are shown in Figure 14. The ESR spectra show the maximum anisotropy of ^{31}P ($a_{P\parallel}$) to be perpendicular to this axis, indicating that the radical *x* axis is coincident with the crystallographic *a* axis. Furthermore the maximum in the anisotropy of ^{35}Cl and ^{37}Cl appears to be parallel with $a_{P\parallel}$, indicating that the direction of $a_{P\parallel}$ corresponds to the orientation of the P–Cl linkage, which is the crystallographic *b* axis in its precursor. From the ESR spectrum of a powdered sample the principal values of a_P and a_{Cl} were obtained. On cooling of the powder sample the ESR parameters remained unchanged. From this it is concluded that radical **8a** has been generated by electron capture rather than by rupture of the P–O linkage. In the latter case the $a_{Cl\parallel}$ and $a_{P\parallel}$ directions should have been expected to be perpendicular. From the ESR data it is derived that $a_{P\text{-}iso}$ = 1317 G, indicating a phosphorus 3s spin density of 0.36. A spin density of 0.40 is located in the phosphorus $3p_z$ orbital as inferred from the anisotropy of a_P. This results in a total spin density of 0.76 on phosphorus. From the ^{35}Cl hfc, one calculates $a_{Cl\text{-}iso}$ = 31 G, indicating a 3s spin density of 0.02, while the anisotropic contribution (*B*) accounts for a spin density of 0.16 in a chlorine $3p_z$ orbital that is directed along the P–Cl linkage. Similar spin densities are obtained from the ^{37}Cl tensor. Therefore, the structure of **8a** is described as C_{4v} with 76% of the unpaired electron located in an axial sp_z hybrid orbital at the phosphorus nucleus and 16% in the $3p_z$ of chlorine.

B. Dynamic Structure. Pseudorotating TBP-e. Octahydro-2a,4a,6a,8a-tetraza-8b-phospha(*8b*-P^V)pentaleno[1,6-*cd*]pentalen-8b-yl Radical. Single crystals of octahydro-2a,4a,6a,8a-tetraza-8b-phospha(*8b*-P^V)pentaleno[1,6-*cd*]pentalen (**5**)[29] were grown by slow crystallization from 1:1 acetonitrile–hexane. The structure of **5** is TBP as revealed by X-ray diffraction analysis.[30]

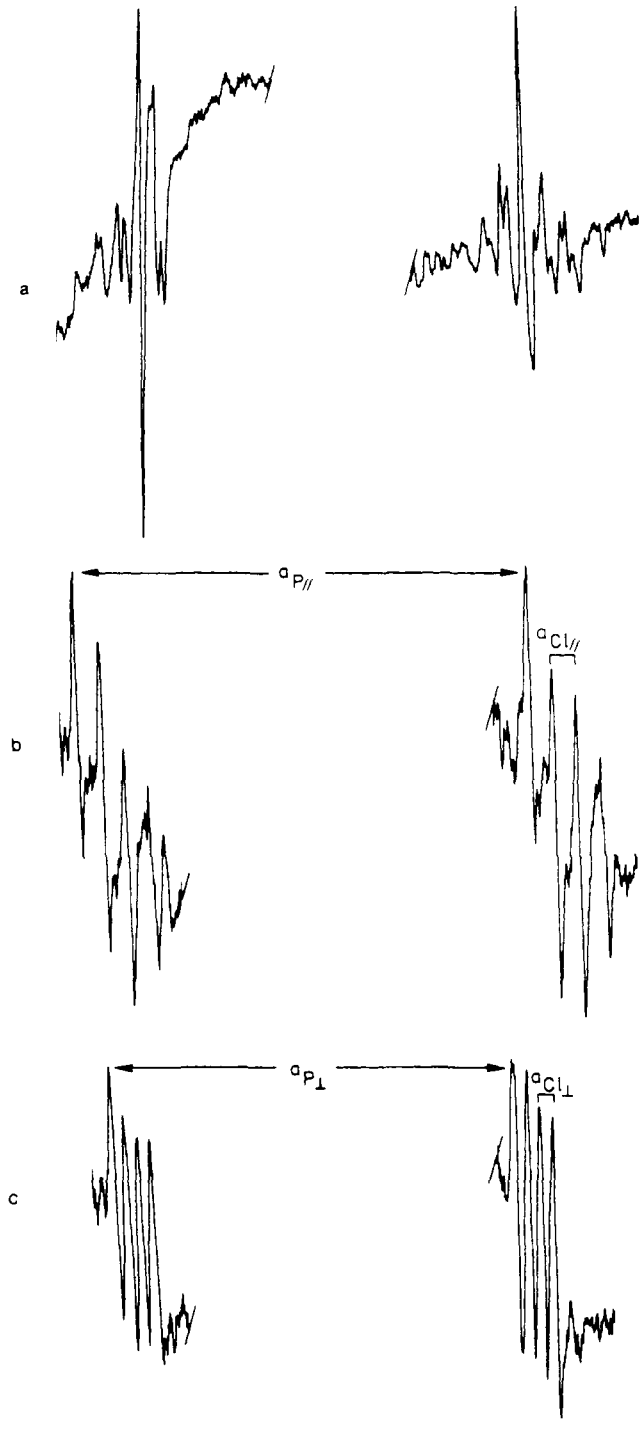

Figure 13. ESR spectra of **8a**: (a) powder spectrum, (b) single-crystal spectrum, H_0 parallel to the *b* axis, (c) single-crystal spectrum, H_0 parallel to the *c* axis.

An ORTEP drawing is given in the Experimental Section. The radical was generated by X irradiation at room temperature and studied between 295 and 258 K. Below 253 K the single crystal became polycrystalline. Powder samples were UV or X irradiated at 77 K and studied between 77 and 295 K.

X irradiation of a powdered sample of **5** at 77 K generated the free hydrogen radical H· (a_H = 509 G). On annealing to 200 K a phosphoranyl radical was detected with $a_{P\parallel}$ = 715 G and $a_{P\perp}$ = 606 G and additional hyperfine coupling $a_{N\parallel}$ = 26.3 G and $a_{N\perp}$ = 24.0 G due to two nitrogen atoms.[31] The principal axis of the ^{14}N hfc is parallel to that of the ^{31}P hfc. From these values one calculates an $a_{P\text{-}iso}$ of 642 G, which indicates a phosphorus 3s spin

(28) Hamerlinck, J. H. H.; Schipper, P.; Buck, H. M. *Chem. Phys. Lett.* **1981**, *80*, 358.
(29) Richman, J. E.; Atkins, T. J. *Tetrahedron Lett.* **1978**, 4333.
(30) The structure determination of **5** was made by Dr. A. Koster of the Department of Physical Chemistry, while the ORTEP drawing was obtained with assistance of Dr. G. J. Visser of the Computing Centre at Eindhoven University of Technology, The Netherlands.
(31) Hamerlinck, J. H. H.; Hermkens, P. H. H.; Schipper, P.; Buck, H. M. *J. Chem. Soc., Chem. Commun.* **1981**, 358.

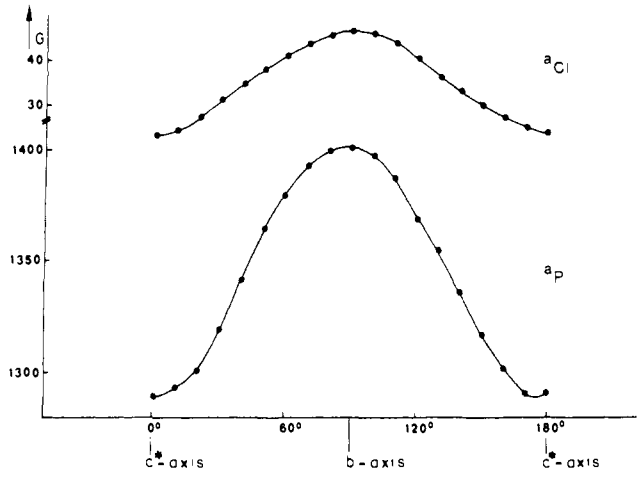

Figure 14. Angular variations of a_P and a_{Cl} of **8a** on rotation around the a axis.

Scheme IV. Pseudorotation of the Radical 5a

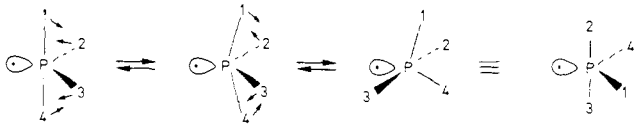

density of 0.18 and a 3p spin density of 0.35, giving a total spin density of 0.53 on phosphorus. The nearly isotropic ^{14}N hfc $a_{N\text{-iso}}$ of 24.8 G indicates a spin density of 0.05 in its 2s orbital. The small anisotropic contribution (0.8 G) can be attributed to a dipole–dipole interaction. From this a TBP-e structure is derived with two apical nitrogen atoms accounting for the observed high hfc and two equatorial nitrogens with small hfc values (<5 G). On further raising of the temperature (to 295 K), an ESR spectrum was obtained that consisted of the same $a_{P\perp}$ and $a_{P\parallel}$ values as found at low temperatures and additional hfc due to four equivalent nitrogen atoms, $a_{N\parallel} = 14.4$ G and $a_{N\perp} = 12.7$ G. These changes in the ESR spectrum are reversible, as indicated by the appearance of the initial spectrum on cooling. Therefore this phenomenon has to be attributed to a rapid pairwise interconversion of the nitrogen ligands.

Additional evidence was obtained by a single-crystal ESR study of **5a**. The ESR spectra of an X-irradiated single crystal of **5** at room temperature show that two identical radicals with an angle between their $a_{P\parallel}$ components of 34 ± 2° are present. These spectra were temperature dependent in the same way as found for the powder sample; at 295 K four equivalent nitrogens were observed, whereas on cooling to 258 K only two nitrogen couplings appeared, with the principal a_P values at exactly the same positions as found at 295 K (Figures 15 and 16). Unfortunately the single crystal became polycrystalline at 253 K, showing the features of the powdered sample with enhanced resolution.

Both the a_P principal values and their directions remain constant throughout temperature variation, indicating that the position of the orbital in which the unpaired electron resides is fixed in this process. Only the ^{14}N hfc varies from 13.3 (4N) to 24.8 G (2N), whereas the anisotropy in ^{14}N hfc is preserved. Furthermore, the process is reversible. From this it is concluded that the nitrogen ligands exchange in a Berry pseudorotation mechanism with the unpaired electron acting as the pivot ($m - 1$).

At low temperature the pseudorotation proceeds more slowly than the measuring frequency of the ^{14}N hfc ($\upsilon = 9 \times 10^7$ Hz), while at room temperature the exchange frequency equals this value, rendering the four nitrogens equivalent. From this, one calculates that $\Delta G^{\ddagger}$ amounts to 6.0 kcal/mol, indicating that the intermediate SP structure lies only slightly above the TBP-e structure. The ligand permutation is given in Scheme IV.

Discussion

Over the last 10 years ESR studies on phosphoranyl P^V radicals have shown that the TBP-e structure is the energetically favored

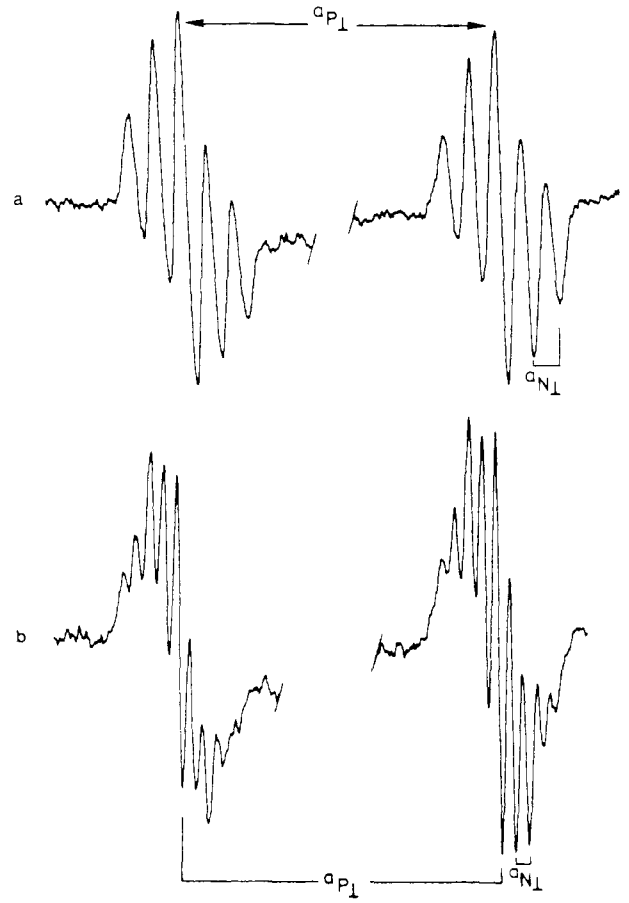

Figure 15. Single-crystal ESR spectra of **5a**: (a) at 258 K, (b) at 295 K.

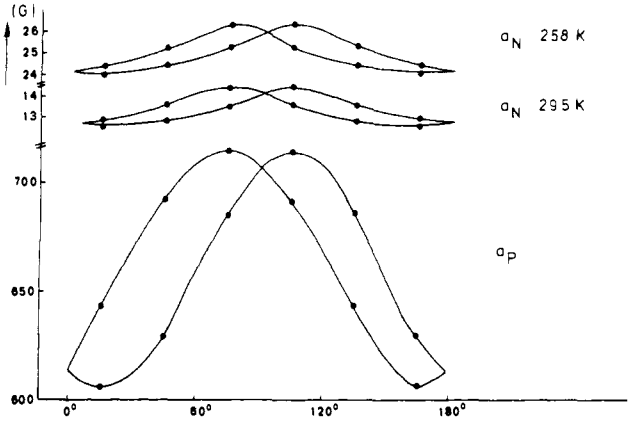

Figure 16. Angular variations of a_P and a_N of **5a**.

one. This was based on the isotropic ^{31}P hfc obtained from liquid-phase ESR and theoretical predictions.[3] In spite of the observation that phosphoranyl radicals in solution are nonrigid, showing ligand exchange, the analogy with the related phosphoranes has not been considered. So it has not been taken into account that phosphoranyl radicals with suitably chosen ligands or ring systems might adopt alternative structures. An indication that the ligands are responsible for the ultimate structure of the radical was found in the ESR spectra of phenylphosphoranyl radicals.[3,32] In the presence of ligands such as OMe and NMe_2, a delocalization of the unpaired electron in the phenyl ligand was found, leading to a tetrahedral configuration for phosphorus.[32] The development of anisotropic ESR studies based on a single-

(32) Boekestein, G.; Jansen, E. H. J. M.; Buck, H. M. *J. Chem. Soc., Chem. Commun.* **1974**, 118.

crystal ESR study of $Cl_3PO^{-}\cdot$[5] and $PF_4\cdot$[6] has opened the possibility for the elucidation of the structure of various organophosphoranyl radicals. For **1a** and **2a** it was found that a single-crystal ESR study in combination with the X-ray diffraction results of the precursor establishes unequivocally that the phosphorus orbital containing the unpaired electron is directed along the initial P–H linkage of the parent hydrocarbon (TBP-e). The usefulness of the method outlined is straightforward and meaningful for comparison of phosphorus compounds even when they are rather different in arrangement. So the TBP-e structure of **1a** and **2a** is in agreement with the assignment of $PF_4\cdot$ in a γ-irradiated single crystal of PF_3.[6] The anisotropic ESR spectrum showed hfc due to one ^{31}P nucleus, two large equivalent fluorine hfc with principal directions perpendicular to the ^{31}P principal values, and two small hfc. From this a TBP-e structure is tentatively deduced with the unpaired electron and the two fluorines with small hfc located equatorially and the two other fluorines in the apical positions. In this case the assignment has been based completely on the directions and magnitudes of the hfc. However, since the radical was produced by addition of F to PF_3, no correlation could be made between the ESR parameters and X-ray analysis. One of the most interesting observations of the single-crystal ESR studies was the determination of a TBP-a structure for **6a** and **7b**. From Table I it is evident that the TBP-e and TBP-a structures exhibit very similar ESR parameters. In fact, the geometries could only be assigned unequivocally because of the availability of the X-ray diffraction results, unless phosphorus bears ligands that have a magnetic moment. Therefore, much of the earlier work on phosphoranyl radicals needs reinvestigation, because invariably in these cases a TBP-e structure was assigned.[33] This structure seems to be supported by the p/s ratio of ~ 2 that is frequently observed. A similar structure was found for $Ph_3PCl\cdot$.[7] It was assumed that in this case the electron spin density resides in the P–Cl antibonding σ^* orbital and that the principal directions of a_P and a_{Cl} are nearly parallel. However, similar spin densities on the apical ligands adjacent to phosphorus have also been observed for TBP-e structures (e.g., $PF_4\cdot$). We presume that the σ^* model, which concerns the excited state of the radical, will be less stable than a TBP-a structure.

The difference in ESR parameters for the TBP-e and TBP-a geometries was visualized for **7a** and **7b**, respectively, both originating from the same precursor (**7**). It appears that the $a_{P\text{-iso}}$ of the TBP-a species is smaller than the corresponding value for the TBP-e. This involves the 3s contribution of phosphorus in the apical location being reduced compared with the equatorial one. A similar trend is found for the analogous phosphoranes. However, the 3s contribution is still so large that structure assignment based on the a_P value without knowledge of the direction of the orbital in which the unpaired electron resides remains questionable.

A P^{VI} structure has been established for **8a**. The directions of maximum values of the magnetic hyperfine tensors of ^{31}P, ^{35}Cl, and ^{37}Cl are coincident and oriented along the P–Cl linkage, indicating an octahedral geometry with the unpaired electron and chlorine in axial positions. The chlorine hfc has a rather large value with respect to the apical chlorine in P^V phosphoranyl radicals.[34] This result opens the interesting possibility of comparison with hexavalent radicals such as $PF_5^{-}\cdot$, $SF_5\cdot$, and $PCl_5^{-}\cdot$. For many years the $PF_5^{-}\cdot$ radical, obtained by γ irradiation of hexafluorophosphate,[9,10] has been thought to be $PF_4\cdot$, which was assumed to rotate rapidly in the matrix, thus accounting for the existence of four equivalent anisotropic fluorines ($a_{F\text{-iso}} = 196$ G) and the isotropic ^{31}P hfc ($a_{P\text{-iso}} = 1346$ G).[35] These values are close to those obtained for the single-crystal irradiated PF_3[6] (vide supra). However, on the basis of a near zero hfc ascribed to a fifth fluorine ligand, it was suggested that the radical center in irradiated hexafluorophosphate should be $PF_5^{-}\cdot$ instead of $PF_4\cdot$.[9] Furthermore, it is believed that the fifth ligand in such C_{4v} geometries possesses an almost zero hfc as a general rule.[10-12] This negligible hfc conflicts with the results obtained for **8a**. Therefore, we suggest that the small coupling detected for $PF_5^{-}\cdot$ is due to a neighboring fluorine in the matrix, as was also the case in TBP-e $PF_4\cdot$.[6] The fact that the phosphorus hfc of the TBP-e $PF_4\cdot$ radical and of the assumed $PF_5^{-}\cdot$ is almost identical, in spite of the higher coordination of the latter one, is also indicative of a P^V phosphoranyl radical (compare **8a** with **4a**; see Table I). On this basis we suggest that there are two possibilities, i.e., the radical center is a pseudorotating TBP-e $PF_4\cdot$, or it is an SP $PF_4\cdot$, vide infra.

Pseudorotation has been observed for **5a**. From the single-crystal ESR analysis it appears that ligand exchange in phosphoranyl radicals proceeds extremely fast in the solid state and that even at low temperature this ligand isomerization takes place. However, if the exchange frequency becomes lower than 9×10^7 Hz, this phenomenon is easily overlooked. This is nicely illustrated with the related radical **9a**, which is generated at 155 K in cyclopropane by UV photolysis of di-*tert*-butyl peroxide in the presence of precursor **9**. The ESR spectrum of **9a** in the liquid

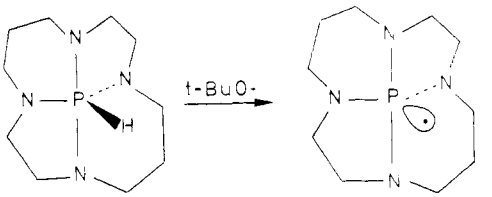

(9) (9a)

phase reveals the presence of an isotropic ^{31}P hfc of 713 G, with hfc due to two nitrogens with $a_N = 27.5$ G indicating a similar TBP-e structure as obtained for **5a**. On warming the radical (**9a**) disappears irreversibly without rendering the four nitrogens equivalent. As a consequence one might have considered this radical as a rigid TBP-e. Unfortunately, the dynamic properties of phosphoranyl radicals are often overlooked in literature. For example, radical **10a** has been characterized as TBP-e with the

(10a) (11a)

NCO ligand in apical position based on the large ^{14}N hfc of 17.4 G and an $a_{P\text{-iso}}$ of 810 G in the liquid phase. Comparison with cyclic analogues[37] exhibiting an $a_N = 26$ G for apical nitrogens and an $a_N = 6.5$ G for equatorial nitrogen results in an averaged value of the ^{14}N hfc of 16 G, which is close to the observed hfc value. Therefore, we suggest that radical **10a** pseudorotates rapidly. In addition, the assignment of a TBP-e structure to **11a** is far from unambiguous since the alternative TBP-a structure with the SR ligand in the equatorial position and the unpaired electron in the apical position, which is a structure close to that of the well-established radical **6a**, is not taken into account.[36] Therefore, the conclusion that was tentatively drawn, that the apicophilicity of the sulfur ligand is more pronounced than that of an alkoxy or trimethylsiloxy group, seems unjustifiable. Generally, we can say that the dynamic properties of **5a** in the single crystal clearly demonstrate that the unpaired electron serves as the pivot in the Berry pseudorotation. Therefore, σ^* intermediates that are suggested in the ligand exchange process of phosphoranyl radicals must be of negative charge.[38] As suggested before, it is plausible that the $PF_4\cdot$ radical observed in irradiated

(33) Dennis, R. W.; Roberts, B. P. *J. Organomet. Chem.* **1973**, *47*, C8.
(34) Schipper, P.; Jansen, E. H. J. M.; Buck, H. M. *Top. Phosphorus Chem.* **1977**, *9*, 494.
(35) Atkins, P. W.; Symons, M. C. R. *J. Chem. Soc.* **1964**, 4363.
(36) Giles, J. R. M.; Roberts, B. P. *J. Chem. Soc., Perkin Trans. 2* **1981**, 1211.
(37) Baban, J. A.; Roberts, B. P. *J. Chem. Soc., Chem. Commun.* **1979**, 537.
(38) Hay, R. S.; Roberts, B. P. *J. Chem. Soc., Perkin Trans. 2* **1978**, 770.

Table II. Atomic Coordinates of 5

atoms[a]	x	y	z
P	0.43 (1)[b]	0.43 (1)	0
N(1)	0.68 (1)	0.30 (1)	0
N(3)	0.44 (1)	0.44 (1)	0.135 (10)
C(5)	0.77 (1)	0.23 (1)	0.08 (1)
C(6)	0.65 (1)	0.35 (1)	0.16 (1)

[a] Atom numbering corresponds to Figure 17. [b] Standard deviations in the last digit are given in parentheses.

hexafluorophosphate undergoes very rapid pseudorotation, rendering the four fluorines equivalent due to the fact that the radical is acyclic. Cooling of the sample to liquid-helium temperature may reveal its TBP-e structure. Another possibility is that it adopts a P^V SP C_{4v} geometry with the unpaired electron localized in the axial position, since it is inferred from the single-crystal ESR study of **5a** that the SP structure is only slightly less stable (6.0 kcal/mol) than the TBP-e structure. In view of results in which both PF_4· and PF_5^-· are observed in the same matrix by irradiation of hexafluorophosphate,[39,40] we propose that the possibility of pseudorotating PF_4· can be ruled out in favor of the SP PF_4· structure, accounting also for the observed small fluorine hfc due to matrix effects. A ligand exchange process possibly accounts for the observed isotropic ^{31}P hfc of Cl_3PO^-· in a single crystal of γ-irradiated Cl_3PO.[5] It is apparent that the isotropic ^{31}P hfc remains incompatible with the results obtained here on phosphoranyl radicals. Therefore, we suggest that the Cl_3PO^-· radical undergoes ligand exchange in such mode that the unpaired electron is not the pivot. Since it is evident from the analysis of the single-crystal spectra of **5a** that the anisotropies of the ligand hfc remain unaffected by the pseudorotation process, the alignment of the anisotropic chlorine hfc due to two apical chlorines does not simply implicate that the Cl–P–Cl angle is 180° but that the angle may deviate dramatically from this value. The same applies for the TBP-e radical PF_4· in irradiated PF_3, where a similar conclusion was made about the axial F–P–F angle.[6] This is clear from inspection of the angular dependence of the hfc of the equatorial fluorines for which the principal hfc is in disagreement with the proposed TBP-e structure, which implies an angle between $a_{F\parallel}$ and $a_{P\parallel}$ of 60°.

Experimental Section

Irradiated crystals, glued on a small quartz rod, were studied on a Varian E-4 X-band ESR spectrometer with a standard Varian cavity equipped with a single-axis goniometer. The angular variation of the a_p's of the various radicals having an axially symmetric system is expressed for any orientation by $a^2 = a_\parallel^2 \cos^2\theta + a_\perp^2 \sin^2\theta$, in which θ is the angle between the $a_\parallel$ component and the applied field. Absorption will occur at all fields between those associated with $a_\parallel$ and $a_\perp$, with the most intense absorption corresponding to $a_\perp$. For convenience, a_P was given in the figures instead of a_P^2. The irradiation experiments were carried out with X-ray or UV laser (λ = 193 or 248 nm). The X-ray crystal structures of the parent compounds are published elsewhere (vide supra) except for **5**. The preparation of the radicals is given in the different sections.

X-ray Structure Determination of 5. The crystals of **5** belong to the tetragonal crystal system with a = 6.102 (7) Å and c = 13.90 (1) Å (numbers in parentheses refer to standard deviations in the last digit). The space group is $P4_2/mnm$ and there are two molecules per unit cell. The calculated density is 1.29 g cm^{-3}. The structure was solved by direct methods with the MULTAN program on the basis of 353 unique reflections. The model could not be refined beyond an R factor of 22%, however, since the crystals show disorder. The coordinates given in Table II refer to a tetragonal cell in which there are four instead of two molecules because of two possible orientations of the molecule. These two orientations are related by a mirror plane through the 2-fold axis of the space group. Electron density maps point also to the possibility that the molecule may be rotated by 90°. Computer drawings are shown in Figure 17. Intramolecular bond distances and angles are listed in Tables III and IV, respectively.

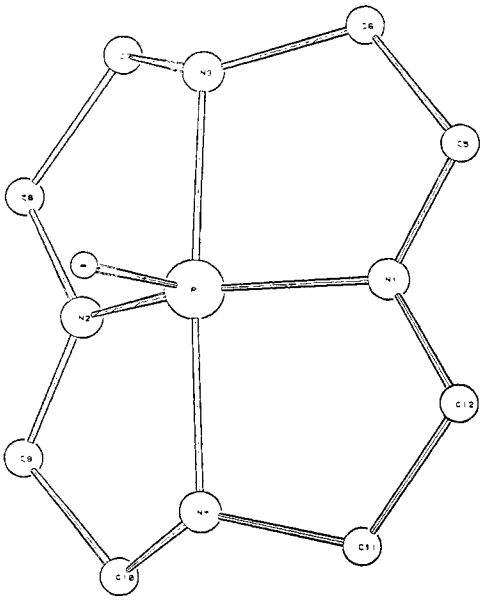

Figure 17. ORTEP drawing of 5.

Table III. Interatomic Distances in 5

atoms[a]	distance, Å
P-N(1)	1.72 (8)[b]
P-N(3)	1.88 (14)
N(1)-C(5)	1.31 (12)
N(3)-C(6)	1.44 (9)
C(5)-C(6)	1.48 (8)

[a] Atom numbering corresponds to Figure 17. [b] Standard deviations are given in parentheses.

Table IV. Bond Angles in 5

atoms[a]	angle, deg	atoms[a]	angle, deg
N(1)-P-N(2)	145 (6)[b]	P-N(1)-C(5)	121 (4)
N(1)-P-N(3)	89 (3)	P-N(3)-C(6)	105 (8)
N(3)-P-N(4)	175 (5)	C(5)-N(1)-C(12)	116 (9)
N(3)-C(6)-C(5)	116 (11)	C(6)-N(3)-C(7)	129 (9)
N(1)-C(5)-C(6)	105 (6)		

[a] Atom numbering corresponds to Figure 17. [b] Standard deviations are given in parentheses.

The N(1)–P–N(2), N(3)–P–N(4), and N(1)–P–N(3) angles in Table IV clearly prove that the configuration of phosphorus is a TBP. It is noticed that the equatorial N(2)–P–N(1) angle of 145° obtained for **5** is the largest one that has been reported for phosphoranes with a TBP structure.

Acknowledgment. This investigation has been supported by the Netherlands Foundation for Chemical Research (SON) with financial aid from the Netherlands Organization for the Advancement of Pure Research (ZWO). We thank Prof. Dr. J. C. Schoone, University of Utrecht, for collecting the X-ray data of **5**.

Appendix

The spin Hamiltonian for a free radical in which one unpaired electron interacts with one nucleus is given by[41]

$$H = \beta\vec{H}\cdot\bar{\bar{g}}\cdot\vec{S} + \vec{S}\cdot\bar{\bar{T}}\cdot\vec{I} - g_N\beta_N\vec{H}\cdot\vec{I}$$

The hyperfine term consists of an isotropic part $a\cdot\vec{S}\cdot\vec{I}$ arising from the Fermi-contact interaction and an anisotropic part $\vec{S}\cdot\bar{\bar{T}}'\cdot\vec{I}$ due to the electron–nuclear dipole interaction. Since phosphorus centered radicals, which show relatively little g tensor anisotropy, are concerned, the simpler Hamiltonian is adopted:

(39) Boate, A. R.; Colussi, A. J.; Morton, J. R.; Preston, K. F. *Chem. Phys. Lett.* **1976**, *37*, 135.
(40) Morton, J. R.; Preston, K. F.; Strach, S. J. *J. Phys. Chem.* **1979**, *83*, 3418.
(41) Carrington, A.; McLachlan, A. D. "Introduction to Magnetic Resonance"; Harper and Row: New York, 1969.

$$H = g\beta\vec{H}\cdot\vec{S} + \vec{S}\cdot\bar{\bar{T}}\cdot\vec{I} - g_N\beta_N\vec{H}\cdot\vec{I}$$

in which g is a scalar. The classical expression for the interaction of an electron moment and a nuclear moment is

$$H_{dip} = -g\beta g_N\beta_N\left\langle\frac{\vec{S}\cdot\vec{I}}{r^3} - \frac{3(\vec{S}\cdot\vec{r})(\vec{I}\cdot\vec{r})}{r^5}\right\rangle$$

In matrix notation:

$$H_{dip} = -g\beta g_N\beta_N[S_xS_yS_z]\begin{bmatrix}\left\langle\frac{r^2-3x^2}{r^5}\right\rangle & \left\langle\frac{-3xy}{r^5}\right\rangle & \left\langle\frac{-3xz}{r^5}\right\rangle\\ \left\langle\frac{-3xy}{r^5}\right\rangle & \left\langle\frac{r^2-3y^2}{r^5}\right\rangle & \left\langle\frac{-3yz}{r^5}\right\rangle\\ \left\langle\frac{-3xz}{r^5}\right\rangle & \left\langle\frac{-3yz}{r^5}\right\rangle & \left\langle\frac{r^2-3z^2}{r^5}\right\rangle\end{bmatrix}\begin{bmatrix}I_x\\ I_y\\ I_z\end{bmatrix}$$

abbreviated as $H_{dip} = \vec{S}\cdot\bar{\bar{T}}'\cdot\vec{I}$.

The condition for diagonalization of $\bar{\bar{T}}'$ is $xy = yz = xz = 0$. This is obtained by choosing $\vec{r}$ along one of the coordinate axes. For an electron in a p_z orbital one obtains

$$T'_{xx} = -(1/2)g\beta g_N\beta_N\langle(3\cos^2\theta - 1)/r^3\rangle$$

$$T'_{yy} = -(1/2)g\beta g_N\beta_N\langle(3\cos^2\theta - 1)/r^3\rangle$$

$$T'_{zz} = g\beta g_N\beta_N\langle(3\cos^2\theta - 1)/r^3\rangle$$

in which θ is the angle between the z axis and the magnetic field direction. Integration over all possible angles for the radius vector to the electron in the p_z orbital and then over all radii r results in

$$T'_{xx} = -(2/5)g\beta g_N\beta_N\langle r^{-3}\rangle = -B_0$$

$$T'_{yy} = -(2/5)g\beta g_N\beta_N\langle r^{-3}\rangle = -B_0$$

$$T'_{zz} = (4/5)g\beta g_N\beta_N\langle r^{-3}\rangle = 2B_0$$

The index $(_0)$ indicates that the spin density is 1 in the p orbital concerned. Therefore, the dipolar contribution is largest and positive along the z axis for an electron residing in the p_z orbital with the magnetic field along the z axis. The complete interaction term $\vec{S}\cdot\bar{\bar{T}}\cdot\vec{I}$ differs only by including the isotropic term $a\cdot\vec{I}\cdot\vec{S}$, so $\bar{\bar{T}}$ is also diagonal in the chosen axis system, with

$$\bar{\bar{T}} = \begin{pmatrix} a + T'_{xx} & & \\ & a + T'_{yy} & \\ & & a + T'_{zz}\end{pmatrix}$$

for an axially symmetric system. It is noted that the dipolar tensor has zero trace, so that $T'_{xx} + T'_{yy} + T'_{zz}$ vanishes and a_{iso} is just the average of T_{xx}, T_{yy}, and T_{zz}. For an electron in a $3d_{z^2}$ orbital similar expressions can be derived.[42] In this case the trace of the dipolar tensor $\bar{\bar{T}}$ consists of

$$T''_{xx} = -(2/7)g\beta g_N\beta_N\langle r^{-3}\rangle$$

$$T''_{yy} = -(2/7)g\beta g_N\beta_N\langle r^{-3}\rangle$$

$$T''_{zz} = (4/7)g\beta g_N\beta_N\langle r^{-3}\rangle$$

in which values are in the same order of magnitude as T'_{xx}, T'_{yy}, and T'_{zz}. Therefore, discrimination between $3p_z$ and $3d_{z^2}$ orbital occupation in the phosphoranyl radicals is not possible, and in this work the anisotropies observed for phosphorus will be considered to arise from 3p contributions only. For an unpaired electron residing in an s orbital on the nucleus the isotropic Fermi-contact contribution is given by

$$a_0 = (8\pi/3)g\beta g_N\beta_N|\psi(0)|^2$$

where the index $(_0)$ indicates that the unpaired spin density is 1 in the s orbital concerned. Since the theoretical values of $|\psi(0)|$ and $\langle r^{-3}\rangle$ are known from Hartree–Fock calculations, it is possible to calculate the isotropic coupling constant a_0 and the anisotropic term B_0 associated with the ns and np orbital, respectively, of each atom. For ^{31}P, $a_0 = 3640$ G and $B_0 = 103$ G.[17] Experimentally, the principal values and directions of the hfc are determined, i.e., the parallel hfc, $a_\parallel$, that is observed when the magnetic field is parallel with the orbital in which the unpaired electron is located and the perpendicular hfc, $a_\perp$. From these principal values the isotropic hfc (a_{iso}), and the anisotropic (B) contribution of the radical under investigation is calculated:

$$a_{iso} = (1/3)(a_\parallel + 2a_\perp)$$

$$B = (1/2)(a_\parallel - a_{iso})$$

These values make it possible to give an estimate of the s character:

$$\rho_s = a_{iso}/a_0$$

and of the p character:

$$\rho_p = B/B_0$$

The results are given in Table I.

Registry No. 1, 67528-51-2; **1a**, 67092-97-1; **2**, 67528-50-1; **2a**, 72314-50-2; **3**, 84142-56-3; **3a**, 84073-98-3; **4**, 181-85-1; **4a**, 72314-51-3; **5**, 64317-97-1; **5a**, 78906-92-0; 6, 73118-93-1; **6a**, 84142-55-2; **7**, 58418-99-8; **7a**/**7b**, 74304-91-9; **8**, 6857-81-4; **8a**, 78509-40-7; **9**, 64317-99-3; **9a**, 84073-99-4; **10a**, 79608-01-8.

(42) Drago, R. S. "Physical Methods in Chemistry"; W. B. Saunders: London, 1977.